AGNAGN seminar
Chapter 14. Active Galactic Nuclei-Results 14.1-3

Taiki Kikuchi

October 17

14.1 Introduction

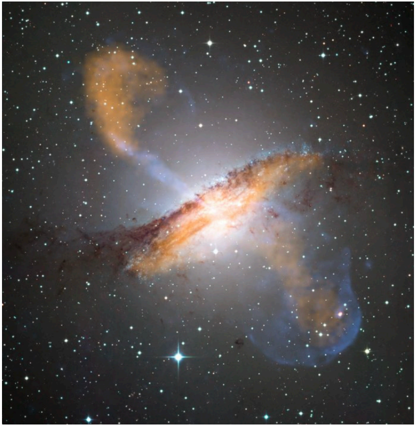

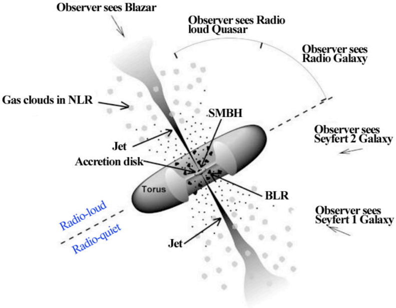

14.1 Introduction

- One of the main features of AGNs is **relatively large portion of high-energy photons**.
- The best current hypothesis of their source : **the immediate surroundings of a black hole**.
- In NLRs(narrow line regions), **the electron densities are comparable** with those in planetary nebulae and HII regions.
- In BLRs, collisional and radiative processes from excited states are not negligible.
- Also resonance lines further complicate the situation in BLRs.

14.2 Energy Source

Let's start with the idea of the energy source of AGNs.

- $L_{\mathrm{AGN}} \simeq 10^{12} L_{\odot} \gg \max L_{\mathrm{star}} = 10^{5} L_{\odot}$
- Thermonuclear reactions cannot produce such extreme luminosity.
- Under the assumption that the system is spherical, its maximum luminosity is given like

$$L \leq L_E = \frac{4\pi c G m_{\mathrm{H}} M}{\sigma_T} = 1.26 \times 10^{38} \frac{M}{M_{\odot}} \tag{1}$$

$$\frac{L}{L_{\odot}} \leq \frac{L_E}{L_{\odot}} = 3.22 \times 10^{4} \frac{M}{M_{\odot}} \tag{2}$$

, which is well known as Eddington luminosity.

14.2 Accretion disk picture

- To achieve AGNs' lumonosity($L \simeq 10^{12} L_{\odot}$) with Eddington maximum luminosity, $M = 3 \times 10^7 \mathrm{M}_{\odot}$ is required.
- Obeservations of BLRs indicate that disk size is about 0.07pc. (very limited volume)
- Thus **large energies** are released in very **small volumes**
- It indicates the rest-mass energy of infalling material can be converted into radiation

  $$L = \eta \dot{M} c^2 \tag{3}$$

  where η is the efficiency of the process.
- **Orbital rotation energy** is also converted into heat.

14.2 AGN spectrum

- As a result, accretion disk model emits a continuum with spectrum

$$L_\nu = C\nu^{1/3} \tag{4}$$

  over a limited range of frequency , with a high-energy exponential cutoff (corresponding to a Planck function $T = 10^{5\sim6}$).
- Actual spectrum deviates from this because of some narrow jet-like plasma structures.
- They are often relativistic and produce high-energy photons mentioned above.

14.2 Model and Observation

Models for ionizing continuum

- The models of the atmosphere of **a hot star** are well constructed.
- But they require detailed information (mass, composition, and age)

Observationally,

- hydrogen-ionizing continuum can be directly observed by selecting higher-redshift objects(like quasors).
- The two portions are fitted for the mean spectrum of ionizing continuum

$$f_\nu \propto \begin{cases} \nu^{-1.76\pm0.12} & 500\mathring{A} < \lambda < 1200\mathring{A} \\ \nu^{-0.69\pm0.06} & 1200\mathring{A} < \lambda < 3000\mathring{A} \end{cases} \tag{5}$$

, where $\lambda = 1200$ corresponds to Lyα.

14.2 Mean continuum of quasars

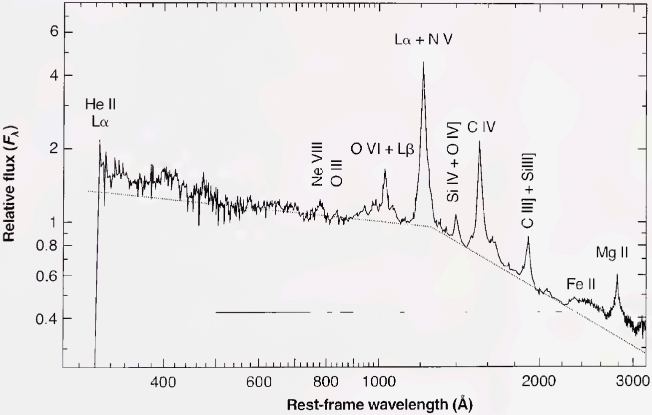

Figure 14.1

The mean continuum from a sample of intermediate-redshift quasars is shown. The dotted line indicates a fitted broken power-law continuum.

14.2 Observation "gap"

There is always a "gap" $912\mathring{A} < \lambda < 25\mathring{A}$.

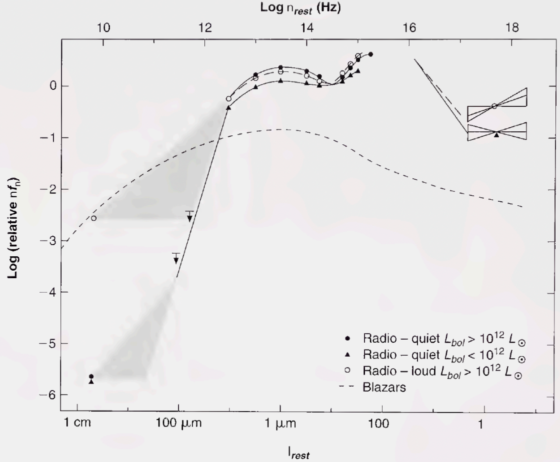

Figure 13.7

Spectral energy distributions for several sets of active nuclei. A horizontal line on this plot corresponds to $L_\nu \propto \nu^{-1}$, and roughly approximates the energy distribution from infrared wavelengths to X-ray energies.

14.2 "gap" interpolation

- The continuum within this gap is very important in photoionizing clouds.
- The simplest approach is to interpolate with Planck function

$$L_\nu = AB_\nu(T_*) \tag{6}$$

- Another way is the use of He. The ionization threshold of He^+ is about $228\mathring{A}$.
- We can estimate the intensity of this line from He II $\lambda 1640$.

14.3 Narrow Line Region

The next step is calculate model AGNs.

- The method is exactly the same as that used in calculating models of planetary nebulae and H II regions(Chapter 5)
- The difference is AGN model includes the additional physical processes relevant for high-energy photons.
- Most of AGNs are not yed spacially resolved. So we assume some kind of symmetry(e.g. spherical, parallel..).

According to Table13.2, 13.4

- The model gives a good representation of the observed spectrum of Cyg A.
- Emission lines ([OI], [SII], [OIII], . . .)are well reproduced.
- A closer look tells us that HeI, HeII, [NI] are predicted too week, which suggest that the **abundance is relatively higher** than expected.

14.3 AGN model spectrum

Required parameters to specify the simplest type of model are $\boldsymbol{f}$(input spectrum), U, n_e, and $\boldsymbol{A}$(set of relative abundance).

$$U = \frac{1}{4\pi r^2 c n_{\mathrm{H}}} \int_{\nu_0}^{\infty} \frac{L_\nu}{h\nu} d\nu = \frac{\mathcal{Q}(\mathrm{H}^0)}{4\pi r^2 c n_{\mathrm{H}}} \tag{7}$$

is the ionization parameter (as previously defined).
Therefore, simplest model spectrum $\boldsymbol{\psi}$ is

$$\boldsymbol{\psi} = \boldsymbol{\psi}(\boldsymbol{f}, U, n_e, \boldsymbol{A}) \tag{8}$$

A more sophisticated model can be built up as a weighted sum of such simple models.

$$\boldsymbol{\Psi} = \sum_i w_i \boldsymbol{\psi}(\boldsymbol{f}, U_i, n_e^i, \boldsymbol{A}) \tag{9}$$

14.3 Diagnosis(refer to fig 14.2, 14.3, 14.4)

In fig14.2, 14.3, 14.4,

- AGNs and HII regions are plotted. AGNs with closed, and HII with open.
- The solid line is empirically derived dividing line between AGNs and HII regions.
- Two short dashed lines indicate model predictions with

$$\alpha = 1.5, \quad n_e = 10^3 \mathrm{cm}^{-3} \tag{10}$$

, where α is the slope of the striking spectrum. The ionization parameter runs from $U = 10^{-2}$ at the upper left, to $U = 10^{-4}$ at the lower right. A means solar abundance, and A' means the abundances of all the heavy elements reduced by a factor ten with respect to H and He.

$$\psi(\alpha = 1.5, U, n_e = 10^3, A), \psi(1.5, U, 10^3, A') \quad (10^{-4} \leq U \leq 10^{-2}) \tag{11}$$

14.3 Diagnosis(refer to fig 14.2, 14.3, 14.4)

- The long dashed line indicates two composite model

$$\Psi = w_1\psi(1.5, U, 10^6, A) + w_2\psi(1.5, U, 10^2, A) \tag{12}$$

- The ratios are chosen to give the best separation.
  - [OIII]/Hβ: an indicator of the mean level of ionization and temperature
  - [OI]/Hα, [SII]/Hα : indicators of high-energy photoionization
  - [NII]/Hα : not so immediately obvious, but it effectively separate AGNs from HII regions.

14.3 Diagnosis Discussion

- The AGN models predict line ratios in the general area.
- The general picture of photoionization by a spectrum that extends to high energies is consistent with the observational data.
- In fig 14.3, 14.4 ([SII], [OI]), most AGNs fall between A and A' ($1 \sim 0.1$ solar abundance).
- On the other hand in fig 14.2 ([NII]), the abundance is higher (about $1.5A$).
- We conclude **N is overabundant** with respect to the other heavy elements in these narrow-line regions of typical AGNs.
- The two component model can be replaced with one simple model with lower abundance $\psi(1.5, U, 10^3, A'' < A)$.
- If we assume $n_e = 10^6 \mathrm{cm}^{-3}$, **collisional deexcitation** becomes weak and thus requires a higher abundance to reproduce the same ratio.

14.3 Overabundant

- Differences in line profiles (Section 14.7) show that these collisional deexcitation effects do occur.
- Hence it is clear that the simple one-component low-density models underestimate the abundances.
- More sophisticated models have been computed and confirm this expectation.

14.3 Other lines

- The two-component models do not predict [FeVII]λ6087, [FeX]λ6375 , which are observed in many Seyfert 2 nuclei.
- This is because this model does not contain very low U.
- Models with a continuous distribution of gas (extending in close to the ionizing source) can reproduce those lines well.

Conclusion

- Photoionization by an assumed hard spectrum seems to explain approximately the observed emission-line intensities. It is the best hypothesis to follow in seeking a complete physical picture of the nature and structure of AGNs